Growth kinetics in a phase field model with continuous symmetry

Umberto Marini Bettolo Marconi
Dipartimento di Matematica e Fisica, Università di Camerino, Istituto Nazionale di Fisica della Materia, Sezione di Camerino, and Istituto Nazionale di Fisica Nucleare, Sezione di Perugia, Via Madonna delle Carceri, I-62032 Camerino, Italy

Andrea Crisanti
Dipartimento di Fisica, Università di Roma ''La Sapienza'' and Istituto Nazionale di Fisica della Materia, Sezione di Roma, Piazzale Aldo Moro 2, I-00185 Roma, Italy

(Received 30 January 1996)

We discuss the static and kinetic properties of a Ginzburg-Landau spherically symmetric O(N) model recently introduced [U. Marini Bettolo Marconi and A. Crisanti, Phys. Rev. Lett. **75**, 2168 (1995)] in order to generalize the so-called phase field model of Langer [Rev. Mod. Phys. **52**, 1 (1980); Science **243**, 1150 (1989)]. The Hamiltonian contains two O(N) invariant fields ϕ and U bilinearly coupled. The order parameter field ϕ evolves according to a nonconserved dynamics, whereas the diffusive field U follows a conserved dynamics. In the limit $N\to\infty$ we obtain an exact solution, which displays an interesting kinetic behavior characterized by three different growth regimes. In the early regime the system displays normal scaling and the average domain size grows as $t^{1/2}$; in the intermediate regime one observes a finite wave-vector instability, which is related to the Mullins-Sekerka instability; finally, in the late stage the structure function has a multiscaling behavior, while the domain size grows as $t^{1/4}$. [S1063-651X(96)06606-8]

PACS number(s): 05.70.Ln, 64.60.Ht, 81.10.Fq, 82.20.Mj

I. INTRODUCTION

When a system described by an order parameter, initially placed into a high-temperature single phase region of its phase diagram, is brought to a point inside the coexistence curve by a sudden change of temperature it becomes thermodynamically unstable and phase separates as a result of the existence of many competing ground states. After the quench the system can order kinetically through either nucleation or spinodal decomposition. In the latter process a microscopic long-wavelength fluctuation initially present is amplified and determines the formation and evolution of various patterns characterized by the presence of a universal length scale $L(t)$, associated with the typical domain size and separation among topological defects. As the system orders, $L(t)$ grows in time in a power-law fashion $t^{1/z}$ and the time-dependent structure factor $C(\boldsymbol{k},t)$ displays dynamical scaling.

A successful approach to the study of these phenomena is represented by the time-dependent Ginzburg-Landau equation. Many years ago Hohenberg and Halperin [1] provided a useful classification of the various models, which comprises a vast class of dynamic critical phenomena, in terms of few parameters. Within their scheme two models have received a great deal of attention: model A, where a single field evolves towards equilibrium with nonconserved order parameter (NCOP) dynamics, and model B, where the order parameter is conserved (COP) [2].

The NCOP dynamics is aimed to describe an ordering process similar to that of the Ising model with conventional Monte Carlo spin flip dynamics, while COP dynamics accounts for the approach to equilibrium of an alloy. In this case, one observes that the system orders by growing droplets larger than a critical size at the expenses of smaller droplets, while keeping the total amount of material fixed. The effect of the conservation law is to slow down the phase separation process, because the material has to be transported via diffusion through the system before being added to a growing region. The value of the dynamical exponent z is $z=2$ for NCOP dynamics, whereas for conserved dynamics it is $z=3$ for a scalar order parameter and $z=4$ for a vector order parameter, indicating that conservation laws play an important role in the dynamic process.

While COP and NCOP dynamics have been widely studied, the phase field model [3], which describes the coupling of a NCOP system with a diffusive COP field such as temperature or concentration, seems not to have been completely explored, in spite of the fact that it displays a variety of interesting peculiar features. To mention only the most striking of these, we recall that the phase field model accounts for the regularity of the shapes observed during the growth of crystals into a supercooled melt. According to the phase field model, a planar solid front growing in the supercooled liquid undergoes the so-called Mullins-Sekerka instability. This phenomenon can be understood as follows. The latent heat, released when the liquid freezes, is diffused into the colder liquid and thus promotes the freezing of more material. The larger the temperature gradient the faster is the advancement of the front. Now, imagine slightly perturbing the isothermal flat solid-liquid interface in a slowly varying fashion. As a result of the deformation, the temperature gradient will be larger on the bulges of such a boundary and thus the heat flux. This makes a solid tip grow faster than a flat portion of interface and provides a mechanism by which perturbation of a finite wavelength is amplified, as discovered by Mullins and Sekerka [4,5].

In a recent Letter [6] we have introduced an N-component version of the phase field model in order to study the evolution of a nonconserved order parameter $\boldsymbol{\phi}$ bilinearly coupled to a conserved field $\boldsymbol{U}$. In the limit $N\to\infty$ we were able to obtain some analytical results on the

nonequilibrium relaxation behavior of the model. Here we expand these results.

The model, inspired by model C [1], displays several interesting features: the evolution of the vector field $\boldsymbol{\phi}$ is nonconserved in the early regime and then after a crossover time it develops an instability at finite wavelength due to the coupling with the conserved field $\boldsymbol{U}$. In the very late regime the COP behavior eventually becomes dominant and $\boldsymbol{\phi}$ shows a genuine COP evolution, including multiscaling. A similar mechanism was reported by Somoza and Sagui [7] in a numerical study of model C, where they observed that, notwithstanding, the nonconserved field evolves faster than the conserved field. For late times the growth is driven by diffusion of the conserved variable and the order parameter becomes slaved by the diffusive field.

The paper is organized as follows. In Sec. II we give a brief physical motivation of the model. The equations defining the model are given in Sec. III and its equilibrium and dynamical properties are discussed in Secs. IV and V, respectively. Finally, Sec. VI contains a brief summary of the results and discussions.

II. MOTIVATION OF THE MODEL

The model we discuss in the present paper belongs to the family of O(N) spherical models and it has been introduced [6] with the aim of studying exactly the coupling of a NCOP field with a diffusive COP field. The O(N) generalization proves to be fruitful because, while retaining the salient features of the phenomena occurring during the diffusion limited growth, it allows for some analytical results in the limit $N\to\infty$.

Historically, models containing couplings quadratic with respect to the material NCOP field ϕ and linear with respect to the COP diffusive thermal field u were introduced as early as the 1970's in the framework of the dynamical critical phenomena and named models C. Later, Langer, in order to study first-order phase transitions accompanied by latent heat of fusion, put forth the so-called phase field model [3], in which the coupling was assumed to be bilinear with respect to the two fields.

The material is characterized by an order parameter ϕ, which assumes a positive value in the solid phase and a negative value in the liquid phase. The local temperature of the system is treated as an additional dynamical field obeying a heat diffusion equation in the presence of sources represented by the amount of material changing phase. The solidification takes place adiabatically so that no heat can flow to the outside. One defines the dimensionless temperature field as $u(\boldsymbol{x},t)=c_p[T(\boldsymbol{x},t)-T_m]/L$, where L is the latent heat of fusion per mole, c_p is the specific molar heat at constant pressure, and T_m is the bulk melting temperature. The spatial average of u at the initial time is the so-called undercooling parameter Δ and is a negative quantity.

The thermal field diffuses according to the modified Fourier equation

$$\frac{\partial u(\boldsymbol{x},t)}{\partial t}=D\nabla^2 u(\boldsymbol{x},t)+\frac{\partial \phi(\boldsymbol{x},t)}{\partial t}, \tag{1}$$

where D is the thermal diffusivity and the last term on the right-hand side is the amount of material that crystallizes per unit time and is thus proportional to the heat released during the first-order transition. Both c_p and D are assumed to be equal in the two phases. The evolution of the order parameter is determined by the nonlinear time-dependent equation of the Ginzburg-Landau type [8–10]:

$$\begin{aligned}\frac{\partial \phi(\boldsymbol{x},t)}{\partial t}&=-\Gamma\frac{\delta}{\delta\phi(\boldsymbol{x},t)}F[\phi,u]\\&=-\Gamma[-\nabla^2\phi+r\phi+g\phi^3+\alpha u].\end{aligned} \tag{2}$$

To describe a two-phase system the form of F is chosen to be a double well for $r<0$. The coupling to the thermal field u can create an unbalance in such a way that for negative values of αu the liquid phase ($\phi\sim-\sqrt{-r/g}$) is metastable with respect to the solid ($\phi\sim+\sqrt{-r/g}$). In the absence of coupling to the temperature field, i.e., $\alpha=0$, Eq. (2) represents the familiar Cahn-Allen equation, also called model A. The process contains two stages: during the first stage the solid grows at the expenses of the liquid, while in the second stage the total amount of solid is nearly constant and the growth is limited by diffusion of the thermal field.

Interestingly, the two dynamical equations (1) and (2) can be derived from a Lyapounov functional $\mathcal{F}$, which plays the role of the time-dependent Ginzburg-Landau potential in the present problem. If one performs the transformation $U=u-\phi$ and eliminates u in favor of the new field U, one can write Eqs. (1) and (2) as

$$\frac{\partial \phi(\boldsymbol{x},t)}{\partial t}=-\Gamma\frac{\delta\mathcal{F}}{\delta\phi(\boldsymbol{x},t)}\bigg|_U, \tag{3}$$

$$\frac{\partial U(\boldsymbol{x},t)}{\partial t}=\frac{D}{\alpha}\nabla^2\frac{\delta\mathcal{F}}{\delta U(\boldsymbol{x},t)}\bigg|_\phi, \tag{4}$$

with the Lyapounov functional

$$\mathcal{F}[\phi,U]=\int d^dx\left[\frac{1}{2}(\nabla\phi)^2+\frac{r}{2}\phi^2+\frac{g}{4}\phi^4++\frac{\alpha}{2}(U+\phi)^2\right]. \tag{5}$$

The functional $\mathcal{F}$ has two equal minima when the temperature field vanishes, i.e., for $U=-\phi$, and generates a complex dynamical behavior, which has been the object of some studies. However, its global properties are not so well known. This leads us to formulate an O(N) invariant vectorial generalization of the above model. This kind of model, in fact, lends itself to nearly analytical solutions, thus providing useful insights on the properties of the scalar order parameter solutions.

III. THE O(N) MODEL

We shall consider a system described by two coupled N-component vector fields $\boldsymbol{\phi}=(\phi_1(\boldsymbol{x},t),\ldots,\phi_N(\boldsymbol{x},t))$ and $\boldsymbol{U}=(U_1(\boldsymbol{x},t),\ldots,U_N(\boldsymbol{x},t))$, whose Hamiltonian can be represented by [11,9]

$$H[\boldsymbol{\phi}(\boldsymbol{x}),\ \boldsymbol{U}(\boldsymbol{x},t)]=\int d^dx\left[\frac{1}{2}(\nabla\boldsymbol{\phi})^2+\frac{r}{2}\boldsymbol{\phi}^2+\frac{g}{4N}(\boldsymbol{\phi}^2)^2+\frac{w}{2}\boldsymbol{U}^2+\mu\boldsymbol{U}\boldsymbol{\phi}\right], \tag{6}$$

where r and g, with $g>0$ and $w>0$, are the standard quadratic and quartic couplings of the Ginzburg-Landau model and the last term represents a bilinear coupling between the field $\boldsymbol{\phi}$ and $\boldsymbol{U}$. The first three terms in Eq. (6) constitute the familiar Ginzburg-Landau-Wilson Hamiltonian describing an O(N) ϕ^4 model, whereas the last two terms represent the interaction between the order parameter field and an external fluctuating field $\boldsymbol{U}$.

We assume that the field $\boldsymbol{\phi}$ evolves according to NCOP dynamics:

$$\frac{\partial\phi_\alpha(\boldsymbol{x},t)}{\partial t}=-\Gamma_\phi\frac{\delta}{\delta\phi_\alpha(\boldsymbol{x},t)}H[\boldsymbol{\phi},\boldsymbol{U}]+\eta_\alpha(\boldsymbol{x},t), \tag{7}$$

whereas the field $\boldsymbol{U}$ is conserved and relaxes according to

$$\frac{\partial U_\alpha(\boldsymbol{x},t)}{\partial t}=\Gamma_U\nabla^2\frac{\delta}{\delta U_\alpha(\boldsymbol{x},t)}H[\boldsymbol{\phi},\boldsymbol{U}]+\xi_\alpha(\boldsymbol{x},t). \tag{8}$$

The noises appearing on the right-hand sides of Eqs. (7) and (8) have zero average and two-point correlations:

$$\langle\eta_\alpha(\boldsymbol{x},t)\eta_\beta(\boldsymbol{x}',t')\rangle=2T_f\Gamma_\phi\delta_{\alpha,\beta}\delta(\boldsymbol{x}-\boldsymbol{x}')\delta(t-t'), \tag{9}$$

$$\langle\xi_\alpha(\boldsymbol{x},t)\xi_\beta(\boldsymbol{x}',t')\rangle=-2T_f\Gamma_U\delta_{\alpha,\beta}\nabla^2\delta(\boldsymbol{x}-\boldsymbol{x}')\delta(t-t'), \tag{10}$$

$$\langle\eta_\alpha(\boldsymbol{x},t)\xi_\beta(\boldsymbol{x}',t')\rangle=0, \tag{11}$$

where T_f is the temperature of the final equilibrium state and Γ_U and Γ_ϕ are the kinetic coefficients.

Introducing the Fourier components of the fields, one can write the evolution equation as

$$\frac{\partial\phi_\alpha(\boldsymbol{k},t)}{\partial t}=F_\phi^\alpha(\boldsymbol{k})+\eta_\alpha(\boldsymbol{k},t), \tag{12}$$

$$\frac{\partial U_\alpha(\boldsymbol{k},t)}{\partial t}=F_U^\alpha(\boldsymbol{k})+\xi_\alpha(\boldsymbol{k},t), \tag{13}$$

where $F_{\phi,U}$ are the Fourier transforms of the first term on the right-hand sides of Eqs. (7) and (8). In the limit $N\to\infty$ the cubic term entering into F_ϕ can be decoupled and we have

$$F_\phi^\alpha(\boldsymbol{k})=M_{\phi\phi}(k,t)\phi_\alpha(\boldsymbol{k},t)+M_{\phi U}(k,t)U_\alpha(\boldsymbol{k},t), \tag{14}$$

$$F_U^\alpha(\boldsymbol{k})=M_{U\phi}(k,t)\phi_\alpha(\boldsymbol{k},t)+M_{UU}(k,t)U_\alpha(\boldsymbol{k},t), \tag{15}$$

where the matrix elements are given by

$$M_{\phi\phi}(k,t)=-\Gamma_\phi[k^2+r+gS(t)],$$

$$M_{\phi U}(k,t)=-\Gamma_\phi\mu,$$

$$M_{U\phi}(k,t)=-\Gamma_U\mu k^2,$$

$$M_{UU}(k,t)=-\Gamma_U w k^2. \tag{16}$$

The quantity $S(t)$ is the integrated $\boldsymbol{\phi}$-structure function

$$S(t)=\frac{1}{N}\sum_{\alpha=1}^{N}\langle\phi_\alpha(\boldsymbol{x},t)\phi_\alpha(\boldsymbol{x},t)\rangle=\int\frac{d^dk}{(2\pi)^d}\langle\phi_\alpha(\boldsymbol{k},t)\phi_\alpha(-\boldsymbol{k},t)\rangle \tag{17}$$

and the integral contains a phenomenological momentum cutoff Λ. The average is over the external noises $\boldsymbol{\eta}$ and $\boldsymbol{\xi}$ and initial conditions.

To study the behavior at finite temperature T_f it is useful to introduce the equations of motion for the three equal-time real-space connected correlation functions $C_{\phi\phi}(r,t)=\langle\phi_\alpha(R+r,t)\phi_\alpha(R,t)\rangle$, $C_{\phi U}(r,t)=\langle\phi_\alpha(R+r,t)U_\alpha(R,t)\rangle$, and $C_{UU}(r,t)=\langle U_\alpha(R+r,t)U_\alpha(R,t)\rangle$, whose Fourier transforms are the structure functions. These correlations are independent of the index α due to the internal symmetry. In the $N\to\infty$ limit the structure functions evolve according to the set of equations

$$\frac{1}{2}\frac{\partial}{\partial t}C_{\phi\phi}(k,t)=M_{\phi\phi}(k,t)C_{\phi\phi}(k,t)+M_{\phi U}(k,t)C_{\phi U}(k,t)+\Gamma_\phi T_f, \tag{18}$$

$$\frac{\partial}{\partial t}C_{\phi U}(k,t)=M_{U\phi}(k,t)C_{\phi\phi}(k,t)+[M_{UU}(k,t)+M_{\phi\phi}(k,t)]C_{\phi U}(k,t)+M_{\phi U}(k,t)C_{UU}(k,t), \tag{19}$$

$$\frac{1}{2}\frac{\partial}{\partial t}C_{UU}(k,t)=M_{U\phi}(k,t)C_{\phi U}(k,t)+M_{UU}(k,t)C_{UU}(k,t)+\Gamma_U T_f k^2. \tag{20}$$

In what follows we shall be more interested in the behavior of the field $\boldsymbol{\phi}$, since it is the relevant order parameter of the system.

IV. EQUILIBRIUM PROPERTIES

In this section we investigate the equilibrium properties of the model (12) and (13). It can be shown that the random process characterized by the Langevin equations (9)–(13) obeys detailed balance since the following ''potential conditions,'' analogous to the Onsager relations, are fulfilled [12]:

$$\frac{\delta}{\delta\phi_\alpha(\boldsymbol{k})}F_\phi^\beta(-\boldsymbol{k}')=\frac{\delta}{\delta\phi_\beta(\boldsymbol{k}')}F_\phi^\alpha(-\boldsymbol{k}), \tag{21}$$

$$\frac{\delta}{\delta\phi_\alpha(\boldsymbol{k})}F_U^\beta(-\boldsymbol{k}')=\frac{\Gamma_U k'^2}{\Gamma_\phi}\frac{\delta}{\delta U_\beta(\boldsymbol{k}')}F_\phi^\alpha(-\boldsymbol{k}), \tag{22}$$

$$\frac{\delta}{\delta U_\alpha(\boldsymbol{k})}F_U^\beta(-\boldsymbol{k}')=\frac{k'^2}{k^2}\frac{\delta}{\delta U_\beta(\boldsymbol{k}')}F_U^\alpha(-\boldsymbol{k}). \tag{23}$$

If detailed balance holds, the stationary probability density reads

$$P_{\rm st}[\boldsymbol{\phi},\boldsymbol{U}]=\mathcal{N}\exp\left(-\frac{1}{T_f}H[\boldsymbol{\phi},\boldsymbol{U}]\right), \tag{24}$$

where $\mathcal{N}$ is a normalization constant.

The equilibrium probability density is quadratic in the field $\boldsymbol{U}$; therefore, as far as the static properties of $\boldsymbol{\phi}$ are involved, the field $\boldsymbol{U}$ can be traced out. One is then left with an effective Hamiltonian for the field $\boldsymbol{\phi}$:

$$H_{\rm eff}[\boldsymbol{\phi}]=\int d^dx\left[\frac{1}{2}(\nabla\boldsymbol{\phi})^2+\frac{r_{\rm eff}}{2}\boldsymbol{\phi}^2+\frac{g}{4N}(\boldsymbol{\phi}^2)^2\right], \tag{25}$$

where $r_{\rm eff}=r-\mu^2/w$ is the ''renormalized mass.'' The importance of the field $\boldsymbol{U}$ can be fully appreciated only in the nonequilibrium dynamics of the system, as will be discussed in Sec. V.

Before considering the dynamics, we briefly discuss the static properties of this model. Unlike the case where the $\boldsymbol{U}$ is quenched [13], the system displays for space dimensions $d>2$ an order-disorder transition when T_f is lower than the critical temperature T_c. In order to locate the critical surface $T_f=T_c(r,g,\mu,w)$ one considers the long-range behavior of the structure functions $C_{\phi\phi}(k)$, which can be computed from (25). The fourth-order term makes the calculation difficult for finite N. However, for $N\to\infty$ we can use the Hartree approximation, exact in this limit, and we readily obtain for $T>T_c$

$$C_{\phi\phi}(k)=\frac{T_f}{k^2+r+gS_\infty-\mu^2/w}, \tag{26}$$

$$S_\infty=\int_{|\boldsymbol{k}|<\Lambda}\frac{d^dk}{(2\pi)^d}C_{\phi\phi}(k). \tag{27}$$

For $T_f\leqslant T_c$ the structure function diverges at small k because the full mass term $r+gS_\infty-\mu^2/w$ vanishes, signaling the appearance of the ordered phase. In fact, the model for $r<\mu^2/w$ and $g>0$ displays a high-temperature paramagnetic phase and a low-temperature ordered phase. The critical temperature is given by the usual form of the ϕ^4 theory $T_c=(\mu^2/w-r)(d-2)/(g\Lambda^{d-2}K_d)$ with $1/K_d=2\pi^{d/2}\Gamma(d/2)$, where $\Gamma(x)$ is the gamma function.

For temperatures T_f below T_c there exists a nonvanishing order parameter $M=\langle\phi_1\rangle$, which can be assumed to be directed along the $\alpha=1$ direction without loss of generality. The $(N-1)$ components of the correlation function orthogonal to the order parameter direction diverge at small k, reflecting the existence of Nambu-Goldstone modes, i.e., excitations of vanishing energy cost in the long-wavelength limit. The real-space two-point correlation function takes the form

$$\langle\phi_\alpha(r)\phi_\alpha(r)\rangle=M^2\delta_{\alpha1}+S_\infty(t), \tag{28}$$

$$M^2=-\frac{1}{g}\left(r-\frac{\mu^2}{w}\right)\left(1-\frac{T_f}{T_c}\right), \tag{29}$$

where S_∞, defined in Eq. (27), comes from the transverse components only.

The other equilibrium correlation functions can also be obtained from the stationary equilibrium distribution and read for $T>T_c$

$$C_{UU}(k)=\frac{T_f}{w-\mu^2(k^2+r+gS_\infty)^{-1}}, \tag{30}$$

$$C_{\phi U}(k)=-\left(\frac{\mu}{w}\right)\frac{T_f}{k^2+r+gS_\infty-\mu^2/w}. \tag{31}$$

Note that both $C_{\phi U}(k)$ and $C_{UU}(k)$ are singular for $k\to0$.

We conclude by noting that to obtain the static structure functions from the dynamical equations one has to supplement the requirement that the right-hand sides of Eqs. (18)–(20) vanish with the stronger condition

$$\lim_{t\to\infty}[M_{U\phi}(k,t)C_{\phi\phi}(k,t)+M_{UU}(k,t)C_{\phi U}(k,t)]=0, \tag{32}$$

$$\lim_{t\to\infty}[M_{\phi\phi}(k,t)C_{\phi U}(k,t)+M_{\phi U}(k,t)C_{UU}(k,t)]=0 \tag{33}$$

to ensure that the equilibrium properties of the model are independent on the kinetic coefficients Γ_ϕ and Γ_U. The conditions (32) and (33) can also be deduced from the equilibrium properties of the model (see the Appendix).

V. DYNAMICAL PROPERTIES

Since the behavior at $T_f=0$ is representative of the entire dynamics in the ordered phase when $T_f<T_c$, we shall neglect the noise terms in the following analysis [2]. For general initial conditions the two fields are not in equilibrium and we may expect that the relaxation of $\boldsymbol{\phi}$ is only slightly modified by the external field $\boldsymbol{U}$. Since the dynamics of $\boldsymbol{U}$ is sufficiently slow compared to that of $\boldsymbol{\phi}$, the presence of $\boldsymbol{U}$ does not modify qualitatively the NCOP behavior of $\boldsymbol{\phi}$. In particular, the size of the domains of $\boldsymbol{\phi}$ should grow with a characteristic length $L(t)\sim t^{1/2}$, while the maximum of the structure factor is located at $k=0$ and should increase in time with the power $t^{d/2}$.

This kind of behavior persists until the domain size reaches the typical length associated with the field $\boldsymbol{U}$ and is given by the maximum of the structure function of $\boldsymbol{U}$. At this stage the dynamics of $\boldsymbol{\phi}$ slows down because the coupling with the conserved field $\boldsymbol{U}$ introduces an additional constraint on the dynamics of $\boldsymbol{\phi}$. For longer times the two fields equilibrate and the COP behavior eventually becomes dominant.

A simple analysis of the equation of motion for $N\to\infty$ gives the scaling of the crossover time with the coupling constant μ. Indeed it is simple to see that making the rescalings

$$t\mu^2\to t,\quad k/\mu\to k,\quad U/\mu\to U,\quad r/\mu\to r,$$
$$g/\mu^{d-1}\to g,\quad \Lambda/\mu\to\Lambda, \tag{34}$$

the parameter μ disappears from the equations of motion for $\phi\equiv\phi_\alpha$ and $U\equiv U_\alpha$:

$$\frac{\partial}{\partial t}\phi(k,t) = -\Gamma_\phi[k^2 + r + gS(t)]\phi(k,t) - \Gamma_\phi \mu U(k,t), \tag{35}$$

$$\frac{\partial}{\partial t}U(k,t) = -\Gamma_U \mu k^2 \phi(k,t) - \Gamma_U w k^2 U(k,t). \tag{36}$$

As a consequence, the crossover time scales as $1/\mu^2$. From this analysis it follows that if the dynamics of U is sufficiently slow, then for $1 \ll t \ll 1/\mu^2$ the field ϕ exhibits a NCOP behavior while for $t \gg 1/\mu^2$ a COP behavior. If the dynamics of U becomes too fast the first NCOP behavior shrinks and becomes hardly observable.

This scenario can be confirmed by solving the equations of motion (35) and (36) in a quasilinear approximation. To this end we assume that

$$R(t) = r + gS(t) \tag{37}$$

is slowly varying in time, so that it can be considered constant over successive intervals of time. In other words, we make a piecewise linearization of the equation of motion along the trajectory. In spite of that, the approximation is sufficient to identify the different regimes of the relaxation process.

If we neglect the time dependence of $R(t)$ and assume it to be nearly constant, Eqs. (35) and (36) become a linear system whose solution has the form

$$\phi(k,t) = c_\phi^+(k)e^{\omega_+(k)t} + c_\phi^-(k)e^{\omega_-(k)t},$$

$$U(k,t) = c_U^+(k)e^{\omega_+(k)t} + c_U^-(k)e^{\omega_-(k)t}, \tag{38}$$

where $\omega_+(k)$ and $\omega_-(k)$ are the eigenvalues of the M matrix,

$$\omega_\pm(k) = \frac{1}{2}[-\Gamma_\phi(k^2+R) - \Gamma_U w k^2 \pm \sqrt{[\Gamma_\phi(k^2+R) + \Gamma_U w k^2]^2 + 4\Gamma_\phi \Gamma_U \mu^2 k^2}]. \tag{39}$$

For time $t \gg 1$ the dynamical behavior of the solution is determined by the larger eigenvalue $\omega_+(k)$. For large k^2, the eigenvalue $\omega_+(k)$ decreases proportionally to $-k^2$ and hence large momenta are exponentially damped. Moreover, we see that $\omega_+(k)$ is a function of k^2, which has either an extremum at $k=0$ or a single maximum for $k=0$, as one can verify by inspecting the small-k behavior of $\omega_+(k)$. The behavior of $\omega+(k)$ is shown in Fig. 1 for $t<\tau_f$ and $t>\tau_f$. The crossover time τ_f is defined as the time when the fastest growing mode moves from $k=0$ to $k\neq 0$. Other definitions of τ_f are possible, e.g., the time when the peak at $k=0$ becomes higher than the $k\neq 0$ one. However, all definitions lead to similar results.

Below the critical temperature T_c and in the early stage of the ordering process the value of $gS(t)$ is small compared with r, i.e., $R<0$, and the larger eigenvalue is well approximated by

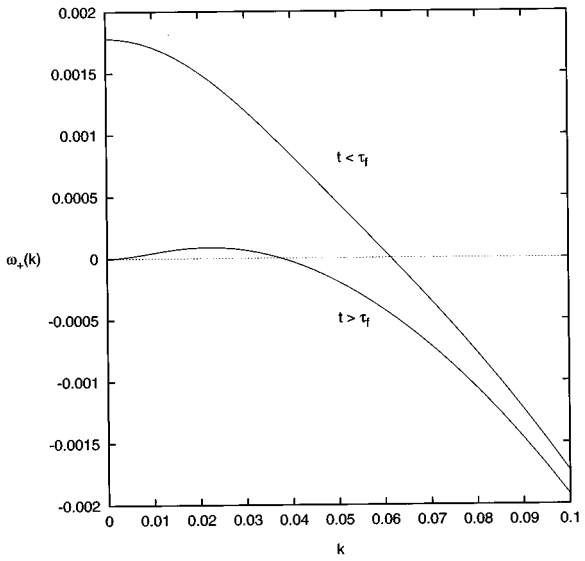

FIG. 1. Dispersion relation $\omega_+(k)$ in the early regime and in the late regime. Both quantities are plotted in arbitrary units. Notice the different long-wavelength behavior in the two cases. The first is typical of NCOP dynamics, whereas the second characterizes COP dynamics.

$$\omega_+(k) = \Gamma_\phi|R| - \left(\Gamma_\phi - \Gamma_U \frac{\mu^2}{|R|}\right)k^2 + O(k^4). \tag{40}$$

A brief calculation reveals that

$$c_\phi^+ = \phi(k,0) + \frac{\mu}{R}U(k,0) + O(k^2), \tag{41}$$

$$c_U^+ = \frac{\Gamma_U \mu}{\Gamma_\phi R}\left[\phi(k,0) + \frac{\mu}{R}U(k,0)\right]k^2 + O(k^4). \tag{42}$$

Therefore, assuming $\phi(k,0) + (\mu/R)U(k,0) = O(1)$ for $k \to 0$, the coefficient $c_\phi^+(k)$ is finite for $k \to 0$, while $c_U^+(k)$ vanishes, indicating that the amplitudes of the longest-wavelength components of U are decreased due to the conservation law.

As a consequence, below T_c the structure factor $C_{\phi\phi}(k,t)$ develops a peak centered at $k=0$, growing in time as a power of t. The structure functions $C_{\phi U}(k,t)$ and $C_{UU}(k,t)$ also develop a peak, centered at a finite value of k, say, k_f, as a result of the competing effect between the k dependence of the exponential factor $\exp[\omega_+(k)t]$ and the amplitude $c_U^+(k)$; see Eq. (42). This mechanism selects a set of exponentially growing U modes with wave vectors in a certain range centered around k_f, whose dependence on the coupling μ is shown in Fig. 2. Such modes represent an inhomogeneity of the U field, which in turn affects the spatial properties of the ϕ subsystem. One witnesses a strong feedback process between the two fields and the outcome is the slaving of the NCOP dynamics of the field ϕ to the COP dynamics of the U field.

The power-law growth of $C_{\phi\phi}(k=0,t)$ can be extracted from the quasilinear approximation by using (40). In the early regime R starts from a negative value and grows towards zero due to the growing of $C_{\phi\phi}(k,t)$ for small k. This

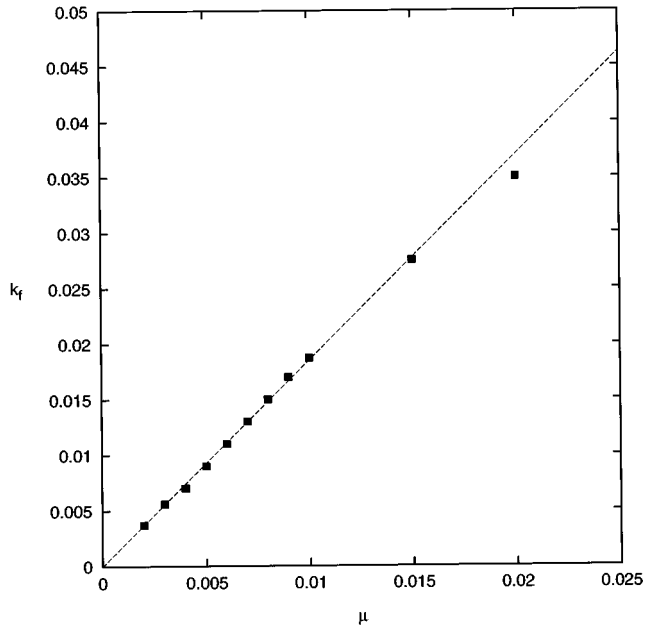

FIG. 2. Dependence of the wave-vector instability k_f on the coupling parameter μ in log-log scale. Both quantities are plotted in arbitrary units. The squares are obtained from the numerical solution of Eqs. (18)–(20) with $\Gamma_\phi=1$, $\Gamma_U=5$, $r=-0.5$, $g=1$, $w=0.05$, and $d=3$. The broken line has slope 1. The value of k_f is taken when the peak at k_f becomes larger than the one at $k=0$. Other definitions, e.g., the fastest growing mode, lead to a similar dependence as follows from the rescaling (34).

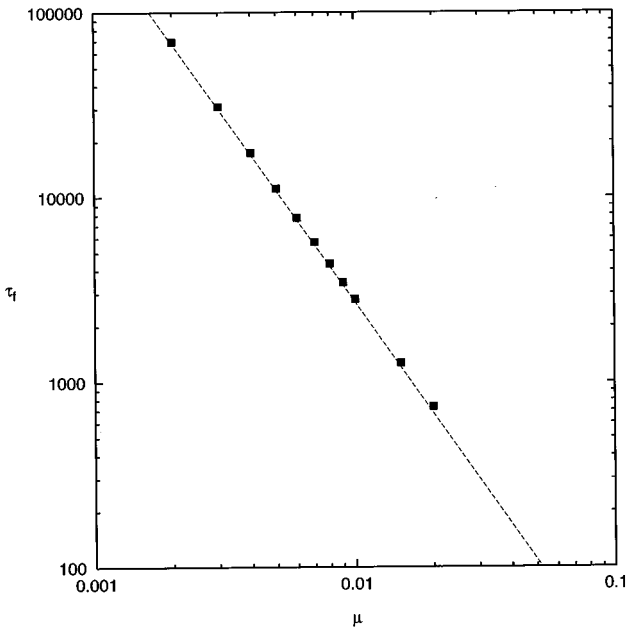

FIG. 3. Dependence of the crossover time τ_f on the coupling parameter μ in log-log scale. Both quantities are plotted in arbitrary units. The broken line has slope -2. The squares are obtained from the numerical solution of Eqs. (18)–(20) with $\Gamma_\phi=1$, $\Gamma_U=5$, $r=-0.5$, $g=1$, $w=0.05$, and $d=3$. The crossover time τ_f is defined as the time when the peak at $k=0$ becomes dominant. Other definitions, e.g., the fastest growing mode, lead to a similar dependence as follows from the rescaling (34).

in turn implies that $S(t)$ tends to a finite value for increasing time. By imposing this condition and making use of (40) it follows that $C_{\phi\phi}(k=0,t)\sim t^{d/2}$, as in the pure NCOP, i.e., the longest-wavelength fluctuations grow faster. We note that while the quasilinear approximation leads to the correct scaling of $C_{\phi\phi}(k=0,t)\sim t^{d/2}$ and of domain size $L(t)\sim t^{1/2}$, it gives $R(t)\sim \ln(t)/t$, which reveals that the approximation is slightly crude.

These results are valid for R/μ^2 not too large, i.e., far from the crossover region where R changes sign. Unlike the pure NCOP, where $R(t)$ goes to zero, after a characteristic time $\tau_f=O(1/\mu^2)$ the value of $|R|$ becomes $O(\mu^2)$ and the NCOP behavior ends. By inspection of Eq. (40) we see that if $|R|/\mu^2<\Gamma_U/\Gamma_\phi$ the maximum of $\omega_+(k)$ moves away from $k=0$ and the system loses its NCOP behavior.

This regime corresponds in our model to the instability that is observed in systems where a nonconserved order parameter is coupled to a conserved field. We must stress that in order to observe the NCOP behavior the dynamics of U needs to be sufficiently slow with respect to the characteristic time $\tau_f\sim 1/\mu^2$, whose dependence on μ is shown in Fig. 3.

For times $t=O(1/\mu^2)$ the quantity R changes sign, becoming positive, and finally, for $t\to\infty$, tends to a finite value μ^2/w while the maximum of $\omega_+(k)$ moves again towards vanishing wave vectors. The dynamics is therefore dominated in the regime $t\gg 1/\mu^2$ by long-wavelength fluctuations. We can then expand $\omega_+(k)$ in powers of k, obtaining

$$\omega_+(k)=\Gamma_U\left(\frac{\mu^2}{r+gS}-w\right)k^2-c_4k^4, \tag{43}$$

where c_4 is a positive coefficient having a finite limit for $\mu^2/R\to w$. By imposing that $S(t)$ has a finite nonzero limit for $t\to\infty$ and making use of Eq. (43), one obtains in this regime

$$C_{\phi\phi}(k,t)=[L(t)^2k_m(t)^{2-d}]^{\varphi[k/k_m(t)]}, \tag{44}$$

where

$$L(t)\sim t^{1/4},\quad k_m(t)\sim\left(\frac{d}{4}\frac{\ln t}{t}\right)^{1/4}, \tag{45}$$

a behavior typical of COP dynamics [14]. The multiscaling function $\varphi(x)$ is given by

$$\varphi(x)=1-(x^2-1)^2. \tag{46}$$

The COP behavior is also observed if one considers the structure functions $C_{\phi U}(k,t)$ and $C_{UU}(k,t)$. Such a multiscaling behavior follows from the competition of two marginally distinct lengths, namely, the domain size $L(t)$ and k_m^{-1}.

Finally, we note that the quasilinear approximation in this regime leads to

$$R(t)-\mu^2/w\sim\left(\frac{\ln t}{t}\right)^{1/2}. \tag{47}$$

From Eq. (26) we see that $R-\mu^2/w$ plays the role of the mass term $r+gS(t)$ in pure COP dynamics [14]; therefore,

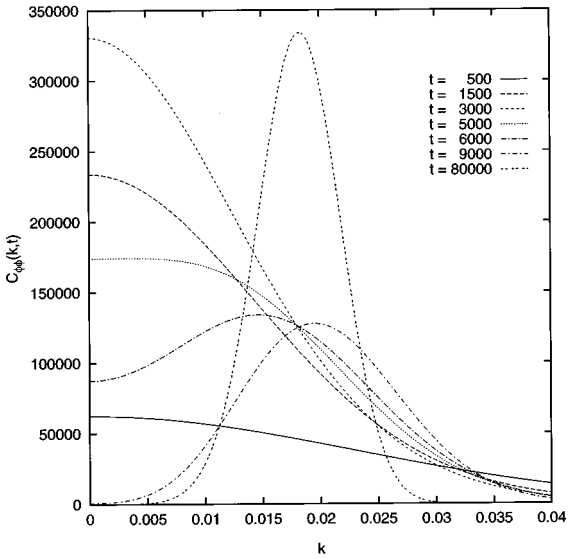

FIG. 4. Typical evolution of the structure function $C_{\phi\phi}(k,t)$ for different times as shown in the figure. Both quantities are plotted in arbitrary units. Notice that the two largest times correspond to $t>\tau_f$ and display the characteristic COP peak. The data are from the numerical solution of Eqs. (18)–(20) with $\Gamma_\phi=1$, $\Gamma_U=5$, $r=-0.5$, $g=1$, $w=0.05$, and $d=3$.

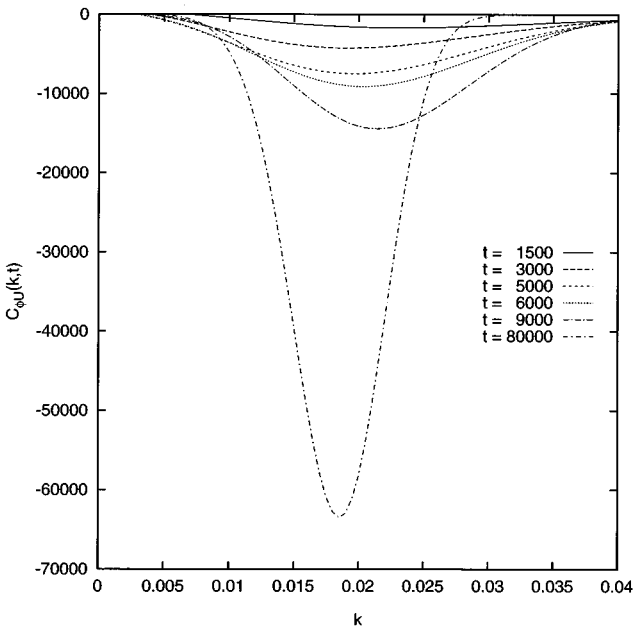

FIG. 5. Typical evolution of the structure function $C_{\phi U}(k,t)$. The data are from the numerical solution of Eqs. (18)–(20) with parameters as in Fig. 4. Both quantities are plotted in arbitrary units.

in spite of the fact that the quasilinear approximation is quite crude, it gives, nevertheless, the correct scaling behavior of COP dynamics.

The above theoretical predictions were checked by integrating numerically the system of equations (18)–(20) by the Euler method. The k integrals were evaluated by a Simpson rule discretizing the wave vectors in the interval $[0,\Lambda]$. Figure 4 displays the structure function $C_{\phi\phi}(k,t)$ for various values of the time t. One clearly sees that in the early regime the fastest growing modes are centered about $k=0$, because long-wavelengths fluctuations of the field ϕ increase more rapidly than shorter ones, whereas for $t>\tau_f$ a finite wave-vector peak appears. Moreover, the growth in this late regime has a conserved character because its value at $k=0$ remains constant. The evolution of $C_{\phi U}(k,t)$ and $C_{UU}(k,t)$ is shown in Figs. 5 and 6. Initially the fields U and ϕ evolve as if they were nearly independent and the C_{UU} correlations display the usual finite wave vector peak of the conserved dynamics, whereas the ϕ field evolves according to a faster nonconserved dynamics. The long-wavelength fluctuations of the $\boldsymbol{U}$ field are hindered by the conservation law and the presence of the $C_{\phi U}$ term has only a small effect on the $C_{\phi\phi}$. However, as the domain size $L(t)$ reaches a critical value and becomes comparable with λ_f, the typical length of the oscillations of the diffusive field, the two fields strongly interact. Within this late regime the dynamics becomes controlled by the conservation law induced by the U field. In Fig. 7 we show the behavior of the height of the peak of $C_{\phi\phi}$ versus time, where one clearly sees the crossover from the early time behavior $t^{d/2}$ to the late stage slope $t^{d/4}$. In the crossover regime due to the presence of a double peak the maximum height decreases until the peak at $k=0$ disappears.

Finally, we report the numerical result concerning the multiscaling observed in the late regime. In Fig. 8 we display the shape function $F(x)=k_m^d(t)C_{\phi\phi}(xk_m,t)$ as a function of x. In Fig. 9 we show the multiscaling function $\varphi(x)$ obtained from the best fit of $C_{\phi\phi}(k,t)$ as a function of $L(t)^2k_m(t)^{2-d}$ for fixed values of $x=k/k_m(t)$. Similar curves can be extracted from the other structure functions. We note that while the data follow quite well the theoretical result (46) for $|x-1|$ not too large, they display a large deviation as $|x-1|$ increases. This is due to the terms neglected in (43). We remark, however, that these become less and less important as k_m decreases; as a consequence, we expect that

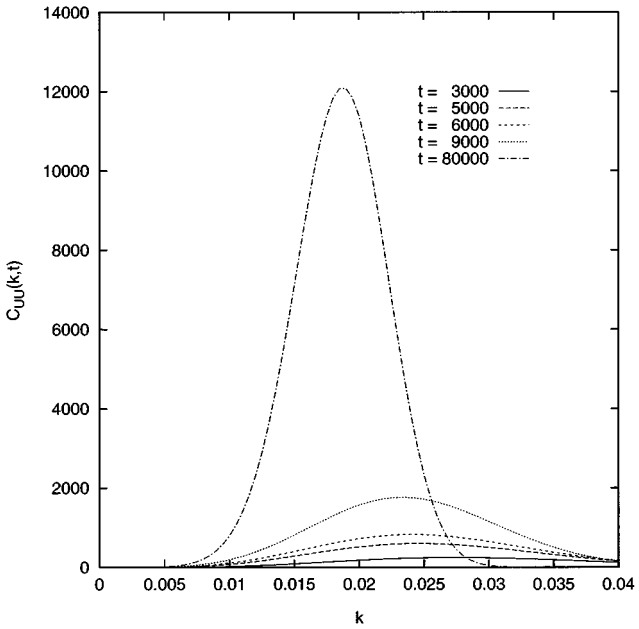

FIG. 6. Time evolution of the structure function $C_{UU}(k,t)$ for different times. Notice the conserved dynamics at all times. The data are from the numerical solution of Eqs. (18)–(20) with parameters as in Fig. 4. Both quantities are plotted in arbitrary units.

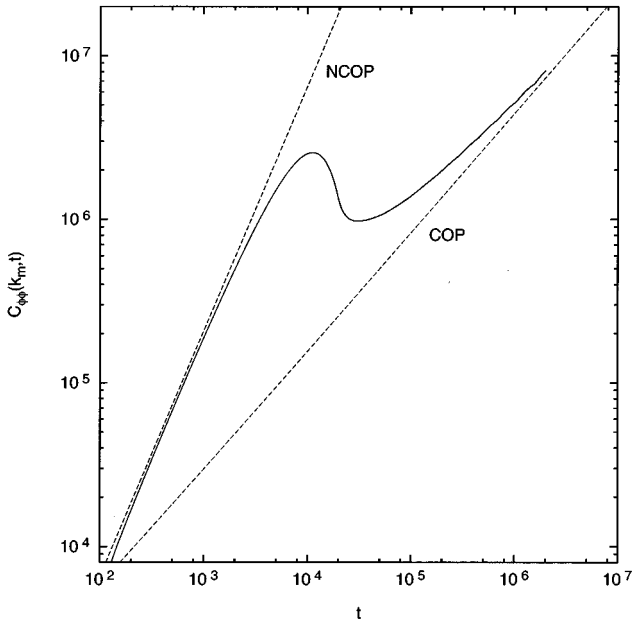

FIG. 7. Height of the peak of the structure function $C_{\phi\phi}(k_m,t)$ as a function of time. Both quantities are plotted in arbitrary units. The crossover from the NCOP behavior to the COP behavior is evident. The dashed line represents the $t^{d/2}$ behavior, whereas the dash-dotted line the $t^{d/4}$ behavior. The data are from the numerical solution of Eqs. (18)–(20) with parameters as in Fig. 4.

the range of values of $|x-1|$ where there is a good agreement with (46) should increase with time. This is indeed observed by using data for increasing time in the best fit. Roughly the range increases as $1/k_m(t)$.

We have explored different types of conservation laws represented by $\Gamma_U k^\mu$ with $0<\mu<2$. In all these cases the dynamics selects for intermediate times a peak at finite values of the wave vector k.

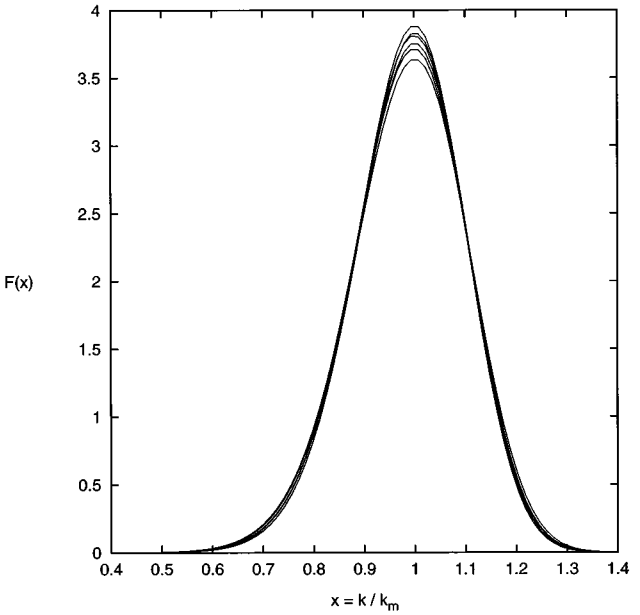

FIG. 8. Shape function $F(x)$ of the $C_{\phi,\phi}(k,t)$ structure function in the late stage evolution. The absence of scaling is evident in figure. The data are from the numerical solution of Eqs. (18)–(20) with parameters as in Fig. 4.

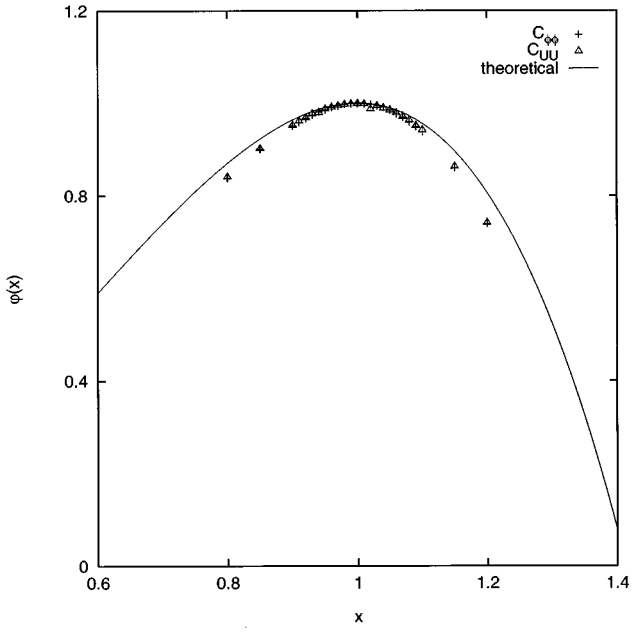

FIG. 9. Multiscaling exponent $\varphi(x)$ defined in the text. The data are from the numerical solution of Eqs. (18)–(20) with $\Gamma_\phi=1$, $\Gamma_U=5$, $r=-0.5$, $g=1$, $w=0.05$, and $d=3$. The crosses are obtained from $C_{\phi\phi}$, while the triangles from C_{UU}. The full line is the theoretical prediction (46).

VI. CONCLUSION

To summarize, in this paper we have studied the evolution of an N-component version of the phase field model and shown that the coupling between the massless transverse modes and the diffusive field produces an instability at finite wavelengths. Our model, where the low-energy Nambu-Goldstone modes couple to the diffusive modes, provides an interesting scenario and we believe represents a paradigm for the Mullins-Sekerka type of phenomena where the soft modes are represented by the capillary wave spectrum associated with the solid-melt interface and the diffusive mode is the heat transport. These two fields concur to destabilize the solid-melt boundary in analogy with our findings. On physical grounds, one expects this kind of instability to occur during phase separation, because small droplets can dissipate heat more efficiently and reach rapidly thermal equilibrium due to the Gibbs-Thomson effect, whereas larger droplets try to dissipate energy faster by creating bulges thus increasing the curvature. As the system cools down upon reaching equilibrium the typical length of the bulges λ_f increases and diverges together with the average domain size $L(t)$. We have demonstrated that the presence of $\boldsymbol{U}$ induces nontrivial effects on the field $\boldsymbol{\phi}$ because it acts on a time scale longer than the noise field, characterized by a short correlation time.

Finally, the O(N) model analyzed presents unusual features since it displays scaling behavior in the early regime ($t<\tau_f$) and multiscaling [15] in the late regime and constitutes an example of multiscaling without COP, a phenomenon that to the best of our knowledge, was not observed before. In summary, the present model reveals an unexpectedly rich dynamical behavior, which, in many respects, is similar to the solidification kinetics.

APPENDIX: EQUILIBRIUM PROPERTIES

In this appendix we shall outline the calculations of the equilibrium properties of the model. The partition function associated with the Hamiltonian

$$Z[\{\boldsymbol{h}(x)\}]=\int_{-\infty}^{\infty}\prod_{\alpha=1}^{N} d\phi_\alpha dU_\alpha e^{-\beta H[\boldsymbol{\phi},\boldsymbol{U}]+\beta \boldsymbol{h}\boldsymbol{\phi}}, \quad \text{(A1)}$$

where we have included an external field $\boldsymbol{h}(\boldsymbol{x})$ coupled linearly to $\boldsymbol{\phi}(\boldsymbol{x})$ and $\beta=(k_B T_f)^{-1}$. The field $\boldsymbol{U}(\boldsymbol{x})$ can be traced out and one finds, apart from uninteresting constants,

$$Z[\{\boldsymbol{h}(x)\}]=\int_{-\infty}^{\infty}\prod_{\alpha=1}^{N} d\phi_\alpha e^{-\beta H_{\rm eff}[\boldsymbol{\phi}]+\beta \boldsymbol{h}\boldsymbol{\phi}}, \quad \text{(A2)}$$

where $H_{\rm eff}$ is defined by Eq. (25). In order to separate the macroscopic component P of the field we employ the identity

$$1=N\int_{-\infty}^{\infty} dP^2\,\delta\left(NP^2-\sum_\alpha \phi_\alpha^2\right) \quad \text{(A3)}$$

and rewrite Z as

$$Z=N\int_{-\infty}^{\infty}dP^2\int_{-\infty}^{\infty}\frac{d\lambda}{2\pi}\int_{-\infty}^{\infty}\prod_{\alpha=1}^{N} d\phi_\alpha \exp\Bigg[-\beta H_{\rm eff}[\phi_\alpha] + \beta \boldsymbol{h}\boldsymbol{\phi}+i\lambda\left(NP^2-\sum_\alpha \phi_\alpha^2\right)\Bigg], \quad \text{(A4)}$$

$$Z=N\int_{\infty}^{\infty}dP^2\int_{-\infty}^{\infty}\frac{d\lambda}{2\pi}\exp\Bigg[-\beta N\left(\frac{r_{\rm eff}}{2}P^2+\frac{g}{4}P^4 - i\frac{\lambda}{\beta}P^2\right)\Bigg]\int_{-\infty}^{\infty}\prod_{\alpha=1}^{N} d\phi_\alpha \exp\Bigg[-\beta/2\sum_\alpha \times\left(-\int d^dx \nabla\phi_\alpha\nabla\phi_\alpha+2i\lambda/\beta\phi_\alpha^2\right)+\beta\sum_\alpha h_\alpha\phi_\alpha\Bigg]. \quad \text{(A5)}$$

In the case of a uniform external field directed along the component 1 ($h_1=h$), after eliminating the ϕ_α fields, Z reads

$$Z=Ne^{(N/2)\ln(2\pi/\beta)}\int_{-\infty}^{\infty}dP^2\int_{-\infty}^{\infty}\frac{d\lambda}{2\pi}e^{N\Omega}, \quad \text{(A6)}$$

$$\Omega=-\beta\int d^dx\left[\frac{r_{\rm eff}}{2}P^2+\frac{g}{4}P^4-i\frac{\lambda}{\beta}P^2\right] - \frac{1}{2}\int\frac{d^dk}{(2\pi)^d}\ln(k^2+2i\lambda/\beta)-i\frac{\beta^2h^2}{4\lambda}. \quad \text{(A7)}$$

In order to evaluate Z we apply the saddle point estimate in the limit $N\to\infty$, imposing the conditions $(\partial Z/\partial\lambda)=0$ and $(\partial Z/\partial P^2)=0$, which lead to the conditions

$$\frac{2i\lambda}{\beta}=r_{\rm eff}+gP^2, \quad \text{(A8)}$$

$$P^2=\int\frac{d^dk}{(2\pi)^d}\frac{1}{k^2+2i\lambda/\beta}-\frac{\beta^2h^2}{4\lambda^2}. \quad \text{(A9)}$$

Eliminating λ with the help of Eqs. (A8) and (A9) we find

$$P^2=\frac{h^2}{(r_{\rm eff}+gP^2)^2}+\frac{1}{\beta}\int\frac{d^dk}{(2\pi)^d}\frac{1}{k^2+r_{\rm eff}+gP^2}=m^2+S_\infty. \quad \text{(A10)}$$

The first term equals m^2, the square of the average magnetization per unit volume $m=(1/V)\,d\ln Z_N/dh$. By using Eq. (A9) we find explicitly

$$m=\frac{\beta}{2i\lambda}=\frac{h}{r_{\rm eff}+gP^2}. \quad \text{(A11)}$$

The existence of a spontaneous magnetic phase implies that in a zero magnetic external field $m\neq0$, i.e., the following condition must be fulfilled:

$$\lim_{h\to0}[r_{\rm eff}+gP^2]=0. \quad \text{(A12)}$$

The equation of state reads

$$\left[r_{\rm eff}+gm^2+gT_f\int\frac{d^dk}{(2\pi)^d}\frac{1}{k^2+r_{\rm eff}+gS_\infty+gm^2}\right]m=h, \quad \text{(A13)}$$

where S_∞ is given by

$$S_\infty=gT_f\int\frac{d^dk}{(2\pi)^d}\frac{1}{k^2+r_{\rm eff}+gS_\infty+gm^2}. \quad \text{(A14)}$$

In order to determine the critical temperature T_c we require $m^2=0$ and $r_{\rm eff}+gS_\infty=0$:

$$T_c=(\mu^2/w-r)(d-2)/(g\Lambda^{d-2}K_d), \quad \text{(A15)}$$

where $1/K_d=2\pi^{d/2}\Gamma(d/2)$, with $\Gamma(x)$ the gamma function.

[1] P. Hohenberg and B.I. Halperin, Rev. Mod. Phys. **49**, 435 (1977).
[2] A.J. Bray, Adv. Phys. **43**, 357 (1994).
[3] J.S. Langer, Rev. Mod. Phys. **52**, 1 (1980); Science **243**, 1150 (1989).
[4] For comprehensive reviews see *Dynamics of Curved Fronts*, edited by P. Pelcé (Academic, New York, 1988); *Solids far from Equilibrium*, edited by C. Godrèche (Cambridge University Press, Cambridge, 1992).
[5] W.L. Mullins and R.F. Sekerka, J. Appl. Phys. **35**, 444 (1964).
[6] U. Marini Bettolo Marconi and A. Crisanti, Phys. Rev. Lett. **75**, 2168 (1995).
[7] A.M. Somoza and C. Sagui, Phys. Rev. E **53**, 5105 (1996).
[8] O. Penrose and P. Fife, Physica D **69**, 107 (1993).
[9] S.L. Wang, R.F. Sekerka, A.A. Wheeler, B.T. Murray, S.R. Corriel, R.J. Braun, and G.B. McFadden. Physica D **69**, 189 (1993).
[10] R. Kupferman, O. Shochet, E. Ben-Jacob, and Z. Schuss, Phys. Rev. B **46**, 16 045 (1992).
[11] J. Collins, A. Chakrabarti, and J.D. Gunton, Phys. Rev. B **39**, 1506 (1989).
[12] R. Graham, in *Quantum Statistics*, edited by G. Höhler, Springer Tracts in Modern Physics Vol. 66 (Springer, Berlin, 1973).
[13] F. de Pasquale, G. Mazenko, P. Tartaglia, and M. Zannetti, Phys. Rev. B **37**, 296 (1988).
[14] A. Coniglio and M. Zannetti, Europhys. Lett. **10**, 575 (1989); A. Coniglio, P. Ruggiero, and M. Zannetti, Phys. Rev. E **50**, 1046 (1994).
[15] A. Coniglio and M. Zannetti, Europhys. Lett. **10**, 575 (1989).